Cell. Mol. Biol. (ISSN: 1165-158X)

Journal Homepage: www.cellmolbiol.org

Cellular and Molecular Biology

Original Article

Unraveling the impacts of progressive drought stress on the photosynthetic light reaction of tomato: assessed by chlorophyll-a fluorescence and gene expression analysis

Saber Nezamivand Chegini[1], Mojtaba Jafarinia[1*], Ali Akbar Ghotbi-Ravandi[2]

[1] Department of Biology, Marvdasht Branch, Islamic Azad University, Marvdasht, Iran
[2] Department of Plant Sciences and Biotechnology, Faculty of Life Sciences and Biotechnology, Shahid Beheshti University, Tehran, Iran

Article Info

Article history:

Received: May 14, 2024
Accepted: November 04, 2024
Published: November 30, 2024

Use your device to scan and read the article online

Abstract

The present study aimed to investigate the impact of progressive drought stress (100%, 75%, 50%, and 25% of field capacity) on photosynthetic light reactions of tomato plants. The imposed drought caused a gradual reduction in leaf RWC leading to a decline in pigment concentration and growth indices. Significant alteration in the OJIP fluorescence transient curves and the formation of specific fluorescence bands (L, K, J, H, and G) gradually increased as drought severity increased. Phenomenological energy fluxes per excited cross-section (ABS/CS, TRo/CS, DIo/CS, ETo/CS and RC/CS) decreased with intensifying drought. As drought stress progressed, JIP-test parameters including The efficiencies of light reactions [φPo/(1- φPo)], the efficiencies of redox reactions [(ψo/(1-ψo)] and the efficiency of PSI to reduce the last electron acceptors [δRo/(1−δRo)] were significantly attenuated. The quantum yields for primary photochemistry (φPo), electron transfer from Q_A to Q_B (ψO), electron transport (φEo), and reduction of end electron acceptors at the PSI acceptor side (φRo) were negatively affected by drought stress. These results indicate that drought progression leads to structural and functional damage in PSII, characterized by a decrease in active reaction centers, reduced energy absorption and trapping, diminished energetic connectivity within PSII, and inhibition of the oxygen-evolving complex. Additionally, reduced plastoquinone pool size, over-reduction of plastoquinone, and impaired redox state downstream of Q_B were observed at the donor side of PSII. The quantum yield and efficiency of PSI to reduce electron acceptors were reduced by drought progression. Our results showed that the transcript levels of *PetE* and *PetF* genes, encoding the key electron careers plastocyanin and ferredoxin, were significantly downregulated in response to an increase in drought severity, contributing to reduced PSI efficiency. The Transcript levels of *PetE* and *PetF* were reduced by 79% and 66% under 25% field capacity treatment, respectively. These results highlight critical points within the photosynthetic apparatus that are highly sensitive to drought, providing valuable insights into the mechanisms of drought-induced damage in tomato plants.

Keywords: Chlorophyll-a fluorescence; JIP-test; *Lycopersicon esculentum*; Photosynthesis; Water stress

1. Introduction

In recent years, the effects of climate change have become more evident, with rising global temperatures and shifting precipitation patterns. The intensification of drought stress is one of the most significant consequences of these changes globally. Climate models predict droughts' frequency, duration, and severity will increase, particularly in arid and semi-arid regions, affecting agricultural productivity. The increased frequency of droughts, associated with the growing global demand for food, seriously threatens agricultural sustainability and food security [1]. Approximately one-third of the global arable land is persistently affected by drought stress, resulting in a considerable reduction in agricultural output [2].

As one of the most important abiotic constraints, drought stress adversely affects several biochemical and physiological parameters in plants, leading to a reduction in growth, yield, and productivity [3]. Drought imposes negative effects on plants including reduced seed germination, stunted growth, decline in nutrient absorption, disruption of metabolic functions, gene expression, protein and misfolding, induction of oxidative stress, and impaired respiration and photosynthesis [4–7]. Photosynthesis is one of the most important physiological processes adversely affected by drought stress due to stomatal and nonstomatal limitations. Reduced stomatal conductance due to a decrease in leaf water potential restricts CO_2 uptake and causes a decline in the rate of carbon fixation [8]. Drought-induced limitations in the Calvin cycle are also linked to a reduction in photosynthetic efficiency by limiting the activity of key enzymes, particularly ribulose-1,5-bisphosphate carboxylase/oxygenase (Rubisco), which becomes

* Corresponding author.
E-mail address: Jafarinia33@gmail.com (M. Jafarinia).
Doi: http://dx.doi.org/10.14715/cmb/2024.70.11.25

less efficient due to lower CO_2 availability and increased photorespiration [9]. Drought stress disrupts the photochemical reaction of photosynthesis, especially the structure and function of the oxygen-evolving complex (OEC), photosystems I and II, and the electron transport chain (ETC) [10]. Limitations in photochemical reactions considerably reduce photochemical efficiency and the quantum yield of plants. The reduced efficiency of the photosynthetic light reactions leads to a decrease in the synthesis of ATP and NADPH, essential cofactors for the Calvin cycle, further limiting the photosynthetic process [11].

While significant progress has been made in understanding the adverse effects of drought stress on photosynthetic machinery, the complexity of photosynthesis, and particularly the intricate nature of photosynthetic light reactions, necessitate further research to fully elucidate the mechanisms underlying drought-induced damage on photochemical reactions, electron transport, and overall performance of light reactions. A comprehensive understanding of these processes is critical for developing effective strategies to mitigate drought impacts on plant productivity. Therefore, the present study aimed to investigate the effects of progressive drought stress on the stability and functionality of photosystems, the efficiency of the photosynthetic electron transport chain, photochemical reactions, and energy utilization and dissipation within the photosynthetic apparatus of tomato plants, as well as exploring the expression of key related photosynthetic genes in response to drought stress.

2. Material and Methods

2.1. Plant Material and Growth Conditions

Tomato seeds (*Lycopersicon esculentum* Mill. var. Peto 86) were sourced from the Plant Improvement Institute of Iran (SPII). To sterilize, seeds were first immersed in 70% ethanol for 2 minutes, followed by a 5-minute exposure to a 6% sodium hypochlorite solution. The seeds were then rinsed with distilled water. Subsequently, the seeds were planted in plastic pots (20 cm in diameter and 25 cm in height) filled with a peat moss and perlite mixture in a 2:1 volume ratio. The pots were placed in a growth chamber with controlled conditions of temperature (25 ± 2°C), humidity (60 ± 5%), and a photoperiod (16 hours of light followed by 8 hours of darkness). Once germination occurred, the seedlings were thinned to one plant per pot.

2.2. Drought Stress Treatment

Tomato seedlings were cultivated in 100% soil field capacity (FC) until the four-leaf stage (30 Days). Drought stress was induced by withholding water until the soil moisture levels reached 75%, 50%, and 25% of FC for 30 days, based on the following formula. The control group continued to receive normal irrigation. Sampling was performed one month after imposed drought stress on the youngest fully expanded leaves.

FC (%) = (Soil fresh weight – soil dry weight /Soil dry weight) × 100.

2.3. Determination of leaf relative water content (RWC)

To determine RWC, leaf samples' fresh weight (FW) was recorded. To measure turgid weight (TW), plant samples were submerged in distilled water for 16 hours in darkness at room temperature to obtain full turgor pressure. After rehydration, excess surface water was blotted with filter paper, and the turgid weight was measured. Subsequently, to measure dry weight (DW), plant samples were oven-dried at 70 °C until a constant weight was achieved. The RWC was calculated using the formula: RWC (%) = (FW-DW)/(TW-DW).100.

2.4. Plant growth indices

Plant height, root and shoot fresh weight were measured at harvest. To determine the dry weights, samples were dried at 72 °C for two days and the dry weight was determined by digital scale.

2.5. Measurement of polyphasic chlorophyll-a fluorescence curve and fast fluorescence induction kinetics (JIP-test)

Chlorophyll-*a* fluorescence is a valuable and non-invasive technique commonly employed to evaluate the performance of photosynthetic systems in plants. This method offers important insights into photosynthetic efficiency and the effects of various environmental factors on the photosynthetic apparatus [8]. When dark-adapted plants are illuminated, a characteristic increase in fluorescence intensity, known as the fluorescence transient, is observed. This polyphasic curve consists of four distinct phases: O (indicating the initial or minimal fluorescence), J (representing fluorescence intensity at 2 milliseconds), I (showing fluorescence intensity at 30 milliseconds), and P (denoting maximal fluorescence, typically occurring between 500 to 1000 milliseconds). The JIP-test analyzes the rapid fluorescence kinetics from the chlorophyll-a fluorescence transient, providing a detailed evaluation of the efficiency and performance of photosystems as well as the efficacy of various electron carriers within the electron transfer chain [12]. Table 1 outlines the definitions and calculations of the JIP-test parameters derived from the chlorophyll-a fluorescence transient. Chlorophyll-*a* fluorescence was measured on the youngest fully expanded leaves at room temperature. Prior to experimentation, all leaf samples were dark-adapted for at least 30 minutes. A Handy PEA (Hansatech Instrument Ltd, Lynn, UK) with a high-resolution setting of 10 microseconds was used for the fluorescence measurements. Fluorescence changes during the first second of illumination were detected by high-performance PIN photodiode detectors, and the fluorescence signal was recorded and digitized using a fast analog-to-digital converter in the control unit. The collected data were subsequently analyzed using the Biolyzer 4HP software, developed by the Bioenergetics Laboratory at the University of Geneva, Switzerland.

2.6. Measurement of photosynthetic pigments

Photosynthetic pigments were extracted by homogenizing 100 mg of fresh leaves in 80% ethanol. Following centrifugation, the levels of chlorophyll-a (chl *a*), chlorophyll-b (chl *b*), and carotenoids in the supernatant were quantified using a UV-visible spectrophotometer (CARY 300, Agilent, USA), following the method outlined by [13].

2. 7. RNA extraction, cDNA synthesis and Real-time PCR

A total RNA extraction kit (Sigma-Aldrich, Germany) was employed to isolate RNA from 0.2 g leaf samples. Following extraction, RNA concentration, purity, and in-

Table 1. Abbreviations, formulae, and glossary of selected JIP-test parameters.

Parameter	Explanation
F_0	Minimal fluorescence, when all PSII RCs are open
F_{300} μs	Fluorescence intensity at 300 μs
F_J	Fluorescence intensity at the J-step (2 ms) of OJIP
F_I	Fluorescence intensity at the I-step (30 ms) of OJIP
F_P (F_M)	Maximal recorded fluorescence intensity, at the peak P of OJIP. All PSII RCs are closed.
Ft	Fluorescence at time t after onset of actinic illumination
ABS/CS_m	Absorption flux per CS (at $t = F_m$)
$TR_o/CS_m = \varphi P_o\ (ABS/CS_m)$	Trapped energy flux per CS (at $t = F_m$)
$DI_o/CS_m = (ABS/CS_m) - (TR_o/CS_m)$	Dissipated energy flux per CS (at $t = F_m$)
$ET_o/CS_m = \varphi E_o\ (ABS/CS_m)$	Electron transport flux per CS (at t = F_m)
$\varphi P_o = TR_o/ABS = [1-(F_o/F_m)]$	Quantum yield for primary photochemistry (at $t = F_o$)
ABS/RC = MO (1/VJ) (1/φPo)	Absorption flux (for PSII antenna chlorophylls) per reaction center (RC)
TR_O/RC = MO (1/VJ)	Trapped energy flux (leading to QA reduction) per reaction center RC
ET_O/RC = MO (1/VJ) ψo	Electron transport flux (further than QA^-) per PSII RC (at t = 0)
$DI_O/RC = (ABS/RC) - (TRO/RC)$	Dissipated energy flux per reaction center RC (at t =0)
$\psi_{o=}\ ET_o/TR_o = (1-V_J)$	Quantum yield for electron transfer from Q_A to Q_B (at $t = F_o$)
$\varphi E_o = ET_o/ABS = [1-(F_o/F_m)]\psi_o$	Quantum yield for electron transport (at $t = F_o$)
$\varphi R_o = RE/ABS = TR_o/ABS\ (1-V_I)$	Quantum yield for reduction of end electron acceptors at the PSI acceptor side (at $t = F_o$)
$\varphi P_o\ /(1-\varphi P_o) = [1 - (F_0 / F_M)]/\ 1-[1 - (F_0 / F_M)]$	Efficiencies of light reactions
$\psi_o\ /(1-\psi_o) = (1 - V_J)/1-(1 - V_J)$	Efficiencies of redox reactions
$\delta R_o\ /1-\delta R_o = \varphi P_o \times (VJ/M0) = (ABS/RC)^{-1}$	Efficiency of PSI to reduce the last electron acceptors

Table 2. Genes, accession number, and primer sequences used for quantitative real-time PCR.

Gene	Locus	Primer sequence (5′→3′)	Product size (bp)
Plastocyanin (*PetE*)	Solyc04g082010.1	F: TTCCCACACAACGTCGTA R:GACAGTAACTTTGCCAACCA	194
Ferredoxin (*PetF*)	Solyc03g005190.2	F:TTCCTCACTCACAATGGCAAC R:CCAGCTCTGTAGTTTTACCTT	200
Actin	Solyc11g005330.1.1	F:CATTGTGCTCAGTGGTGGTTC R:TCTGCTGGAAGGTGCTAAGTG	176

tegrity were assessed using NanoDrop™ and RNA electrophoresis. The resulting RNA was treated with DNase I (Promega, USA) to remove any potential genomic DNA contamination. cDNA synthesis was conducted using 2 μg of total RNA and the SuperScript synthesis kit. Primers for *Actin*, *PetE,* and *PetF* were designed using Vector NTI software based on sequences obtained from NCBI (Table 2). The actin gene was utilized as the internal control for normalization. Quantitative real-time PCR was performed using the Corbett Rotor-Gene RG6000 (Corbett Research, Australia). The REST software was employed for the determination of relative gene expression.

2. 8. Data analysis

All experiments were performed with three biological replicates. Data were presented as Mean ± Standard deviation. After confirming the normal distribution of data, the significant differences among treatments were evaluated by one-way analysis of variance (ANOVA) followed by Duncan's post-hoc test, with a level of significance of 95% ($P \leq 0.05$) by SPSS v22 software.

3. Results

3.1. Relative water content and growth indices

Fig.1 depicts the impacts of different water availability conditions on leaf relative water content. The 75% FC treatment caused no considerable change in leaf relative water content in comparison to control plants. However, as drought stress progressed, in 50% and 25% FC treatment, RWC was significantly reduced in tomato leaves compared to the control group ($P<0.05$).

The growth indices of tomato plants were significantly ($p \leq 0.05$) affected by different water availability regimes (Table 3). The root and shoot fresh and dry weights were significantly reduced under 50% and 25% FC, compared to the control group. All levels of water deprivation

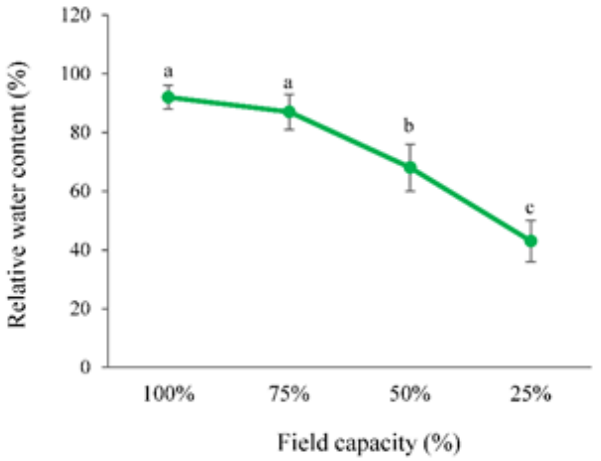

Fig. 1. Changes in the relative water content of tomato plants in response to different water availability conditions including 100%, 75%, 50% and 25% of soil field capacity. Values are the mean of three independent replications. Different letters indicate significant difference (P≤ 0.05).

also significantly affected the root and shoot length. The highest decline in growth indices was observed in the 25% FC treatment.

3.2. Photosynthetic pigments

The effects of drought stress on photosynthetic pigment content are presented in Table 4. The 75% FC did not affect the pigment content of tomato leaves. The content of chl *a*, chl *b*, and carotenoids significantly reduced under 50% and 25% FC compared to the control group. Under 25% FC condition, the content of chl *a*, chl *b*, and carotenoids decreased by 65%, 70%, and 60% respectively, compared to the control.

3.3. Chlorophyll-a fluorescence transient curves and JIP-test parameters

Fig. 2 depicts the OJIP chlorophyll-a fluorescence transient curves of tomatoes in response to progressive drought treatments. The 50% FC treatment led to an increase in the fluorescence intensity at the O and J phases. However, the severe drought (25% FC) resulted in a remarkable decrease in fluorescent intensity at J, I, and P steps (Fig. 2a). In Fig. 2b, the normalized fluorescence transient data was presented to demonstrate the relative variable fluorescence kinetics at any given time. Changes in any different steps of the curve can determine the sites of damage to different electron transport processes. A distinct rise in chlorophyll-a fluorescence intensity at the J and I steps was observed

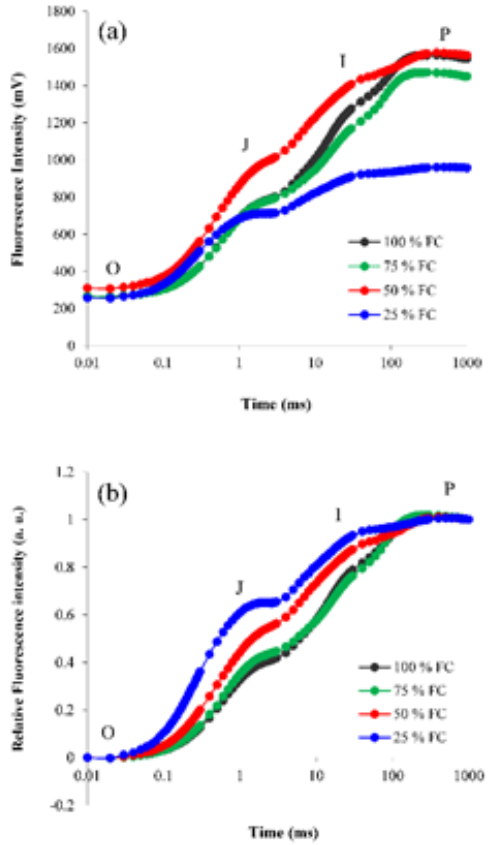

Fig. 2. Fast fluorescence induction curve (a) and its normalized curve between O and P step (b) of tomato seedlings in response to different water availability conditions including 100%, 75%, 50% and 25% of soil field capacity.

Table 3. Effects of different water availability conditions including 100% FC (control), 75% FC, 50% FC, and 25% FC on the growth indices of tomato plants. Values are the mean of three independent replications. Different letters indicate significant difference (P≤ 0.05).

Field Capacity	Shoot fresh weight (g)	Root fresh weight (g)	Shoot dry weight (g)	Root dry weight (g)	Shoot length (cm)	Root length (cm)
100 %	35.23 ± 1.3 a	14.51 ± 1.22 a	4.24 ± 0.35 a	1.05 ± 0.14 a	19.42 ± 1.03 a	9.82 ± 1.07 a
75 %	36.44 ± 1.09 a	13.22 ± 0.98 a	4.92 ± 0.59 a	0.96 ± 0.09 a	17.18 ±1.14 b	7.88 ± 0.95 b
50 %	27.43 ± 1.29 b	9.21 ± 1.06 b	2.38 ± 0.21 b	0.88 ± 0.11 b	14.27 ± 1.45 c	5.34 ±1.28 c
25 %	17.12 ± 1.24 c	6.82 ± 0.93 c	1.41 ± 0.43 c	0.71 ± 0.07 c	9.44 ± 1.09 d	3.64 ± 1.17 d

Values are the mean of three independent replications. Different letters indicate significant difference (P≤ 0.05).

Table 4. Effects of different water availability conditions including 100% FC (control), 75% FC, 50% FC, and 25% FC on the photosynthetic pigments of tomato plants.

Pigment	Content (µg g^{-1} DW)			
	100 % FC	**75 % FC**	**50 % FC**	**25 % FC**
Chlorophyll-a	1.50 ± 0.19 a	1.55 ± 0.13 a	0.93 ± 0.13 b	0.52 ± 0.15 c
Chlorophyll-b	0.62 ± 0.05 a	0.68 ± 0.07 a	0.49 ± 0.08 b	0.18 ± 0.06 c
Carotenoids	0.78 ± 0.04 a	0.71 ± 0.08 a	0.55 ± 0.06 b	0.31 ± 0.05 c

Values are the mean of three independent replications. Different letters indicate significant difference (P≤ 0.05).

in 50% and 25% FC-treated plants compared to the control group. As drought stress intensified, the increase in fluorescence intensity at the J and I steps became more pronounced, with the most significant rise observed at 25% field capacity (FC).

The L-band (Fig. 3a) was visualized by normalization of relative fluorescence between O and K steps [W_{OK}= (Ft−Fo)/(F_K−Fo)] [W_{OI}= (Ft−FJ)/(F_I−FJ)]. The L-band was formed under 50% and 25% FC treatments. The K-band was visualized by the normalization of fluorescence intensity between O and J steps [W_{OJ}= (Ft−Fo)/(F_J−Fo)] (Fig. 3b). The induced water stress of 50% and 25% FC led to the rise in the K-band. The normalization of the relative fluorescence between O and I steps [W_{OI}= (Ft−Fo)/(F_I−Fo)], visualized the J-band (Fig. 3c). The J band was heightened under different levels of drought stress. To visualize the H-band, fluorescence intensity between J and I steps was normalized steps [W_{OI}= (Ft−FJ)/(F_I−FJ)]. The imposed 50% and 25% FC stress caused a significant rise in the H-band as compared to the control group (Fig. 3d). To examine the G-band, we normalized the relative fluorescence between I and P steps (Fig. 3e). Drought stress caused a rise in the H-band in 50% and 25% FC treatments, as compared to the control group. The most pronounced L-band, K-band, J-band, H-band, and G-band were observed in 25% of FC treatments.

Effects of imposed drought stress on energy fluxes per cross-section (CS) are depicted in Fig. 4. Parameters corresponding to the CS, including absorption flux (ABS/CS), trapped energy (TRo/CS), dissipated energy (DIo/CS), electron transport (ETo/CS), and active reaction centers (RC/CSm) were negatively affected by severe drought levels stress in tomato seedlings, as compared to the control group.

Fig. 5. depicts the impacts of different water availability regimes on the efficiency of light reactions [φPo /(1-φPo)], the efficiency of redox reactions [(ψo /(1- ψo)],

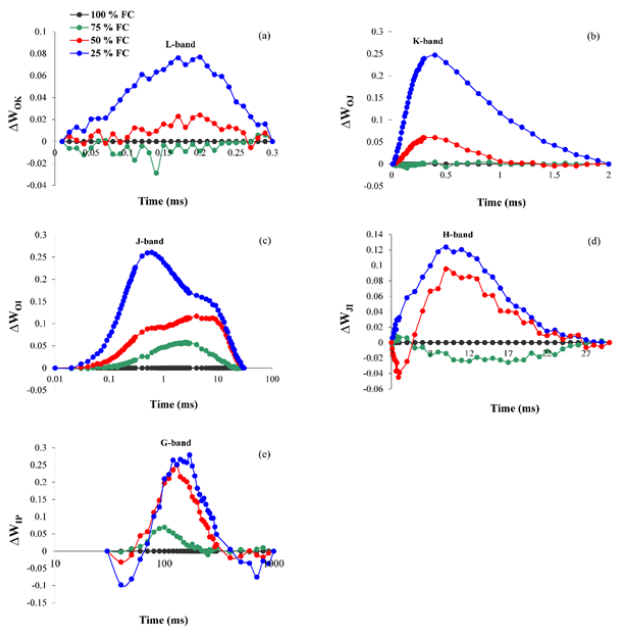

Fig. 3. Effects of different water availability conditions including 100% FC (control), 75% FC, 50% FC, and 25% FC on the formation of L-band (a), K-band (b), J-band (c), H-band (d), and G-band (h) in tomato plants.

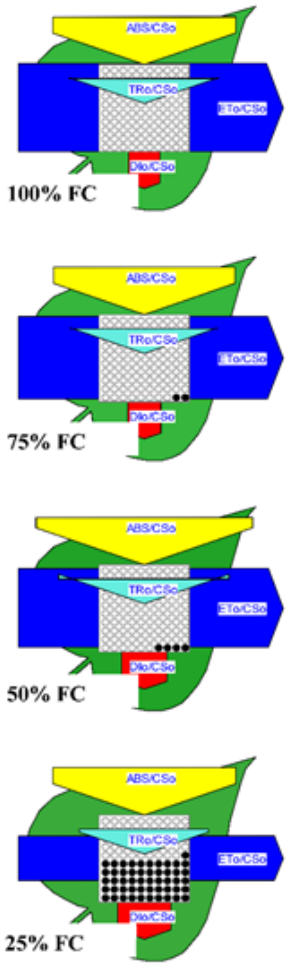

Field Capacity	JIP Parameters				
	ABS/CS	TRo/CS	ETo/CS	DIo/CS	RC/CS
100%	379^a	329^a	141^a	50^c	191^a
75%	378^a	325^a	132^b	53^c	187^{ab}
50%	330^b	261^b	125^c	69^b	183^b
25%	281^c	199^c	73^d	82^a	94^c

Fig. 4. Phenomenological flux parameters per excited cross-section (CS) in tomato plants under different water availability conditions including 100% FC (control), 75% FC, 50% FC, and 25% FC. The data for each parameter are presented in the table. Different letters indicate significant difference (P≤ 0.05).

and the efficiency of PSI to reduce the last electron acceptors [δRo/(1−δRo)]. The 50% and 25% FC treatment led to a significant decrease in all the efficiencies in tomato plants compared to the control group. The efficiency of redox reactions was more sensitive to the imposed water deprivation levels and the value of [(ψo /(1- ψo)] reduced by 11%, 43%, and 66% in response to 75%, 50%, and 25% FC, respectively.

To further analyze the impacts of drought stress on components involved in the efficiency of redox reactions, several parameters including the quantum yield for primary photochemistry (φPo), the quantum yield for electron transfer from Q_A to Q_B (ψ_O), the quantum yield for electron transport (φEo), the quantum yield for the reduction of end electron acceptors at the PSI acceptor side (φRo), and the probability of electron transport from reduced plastoquinone to the acceptor site of PSI (δRo) were determined (Fig. 6). The imposed drought led to significant decrease

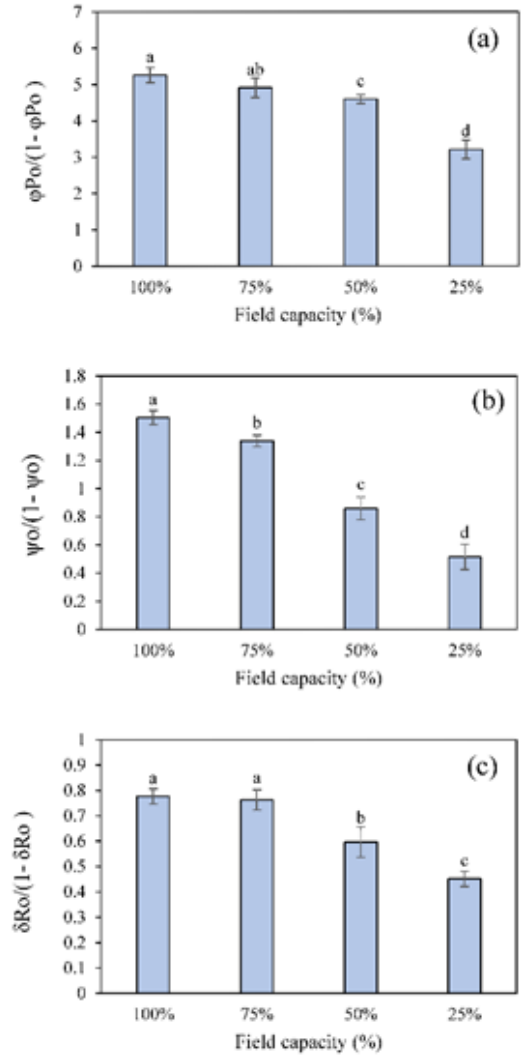

Fig. 5. Changes in efficiency of light reactions [φPo /(1- φPo)], the efficiency of redox reactions [(ψo /(1- ψo)], and the efficiency of PSI to reduce the last electron acceptors [δRo/(1−δRo)] of tomato plant in response to different water availability conditions including 100% FC (control), 75% FC, 50% FC, and 25% FC. Values are the mean of three independent replications. Different letters indicate significant difference (P≤ 0.05).

in value of φPo, $\psi_{O,}$ φEo, φRo, and δRo. Among these parameters, the quantum yield for primary photochemistry was less affected by different levels of water availability compared to the other parameters. On the other hand, the quantum yield for the reduction of end electron acceptors at the PSI acceptor side was the most sensitive parameter to progressive drought stress, since the value for φRo reduced 46% and 72% in response to 50%, and 25% FC, respectively.

3.4. Expression pattern of photosynthetic genes

The transcript levels of the genes *PetE* and *PetF* were significantly affected by the imposed drought stress (Fig. 7). The expression levels of *PetE* were significantly decreased by 57% and 79% under 50% and 25% FC, respectively. Similarly, the transcript levels of *PetF* reduced significantly by 15%, 42%, and 66% in response to 75%, 50%, and 25% FC, respectively.

4. Discussion

Drought is widely recognized as one of the most harmful environmental stresses, significantly limiting plant growth and reducing agricultural productivity on a global scale. As drought stress progresses, a gradual reduction in

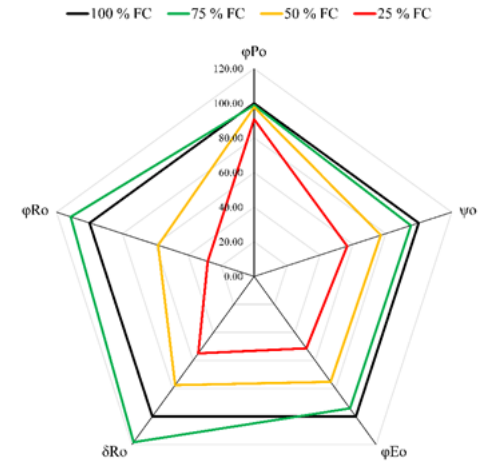

Fig. 6. Changes in the quantum yield for primary photochemistry (φPo), the quantum yield for electron transfer from Q_A to Q_B (ψ_O), the quantum yield for electron transport (φEo), the quantum yield for the reduction of end electron acceptors at the PSI acceptor side (φRo), and the probability of electron transport from reduced plastoquinone to the acceptor site of PSI (δRo) of tomato plant in response to different water availability conditions including 100% FC (control), 75% FC, 50% FC, and 25% FC.

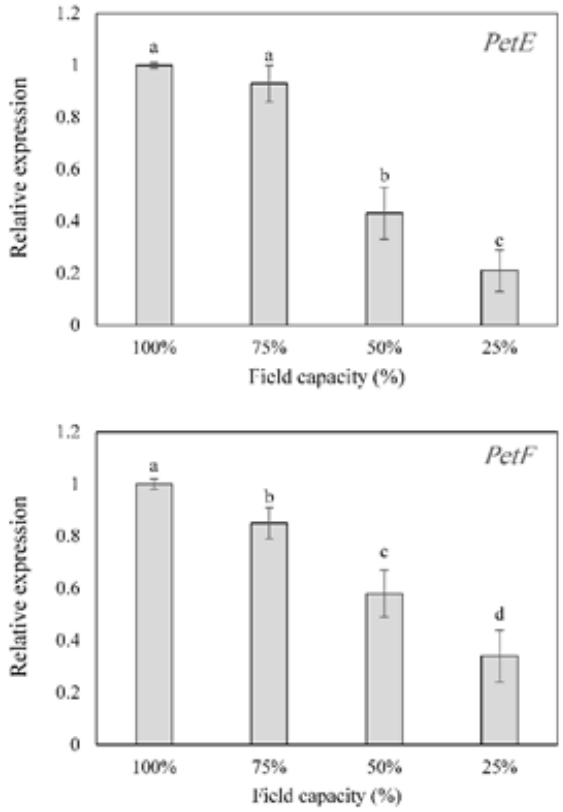

Fig. 7. Effects of different water availability conditions including 100% FC (control), 75% FC, 50% FC, and 25% FC on the relative expression of PetE and petF genes. Values are the mean of three independent replications. Different letters indicate significant difference (P≤ 0.05).

RWC results in a decline in turgor pressure. Since cell expansion and growth are turgor-dependent, these processes are severely affected by drought stress [14]. In the present study, the growth indices of tomato plants showed a significant decline, coinciding with a reduction in RWC as drought stress intensified. Impairment of photosynthesis and limitations in the photosynthetic products can also contribute to the lower growth rate under drought.

Photosynthesis is at the frontline when plants are experiencing drought stress. Leaf pigmentation is very responsive to environmental factors and serves as a key indicator of a plant's photosynthetic efficiency and stress tolerance. Under drought conditions, the levels of photosynthetic pigments (chlorophyll-a,*b,* and carotenoids), often decrease, leading to a decline in the plant's ability to capture light energy efficiently [15]. Drought-induced production of reactive oxygen species (ROS) can accelerate the degradation of chlorophyll and other pigments. Furthermore, drought stress disrupts the synthesis of chlorophyll by affecting the enzymes involved in its biosynthetic pathway [16]. In this study, the chlorophylls and carotenoid content in tomato leaves significantly decreased as drought stress progressed. Similar to our results, [15] reported a significant reduction in the pigment content of cabbage in response to drought stress advancement. Similarly, the decline in the chlorophylls and carotenoid content was also reported in potato leaves in response to drought stress [17].

To evaluate the impacts of the progressive drought on the photosynthetic light reaction integrity and efficiency of tomatoes, polyphasic chlorophyll-a fluorescence was used. Chlorophyll-a fluorescence transients reflect the sequential reduction of electron carriers in the electron transport chain and are characterized by four distinct phases, labeled O, J, I, and P. Each of these phases corresponds to a specific stage of photosynthetic electron transfer, providing insights into the efficiency and dynamics of the process [18]. In the O step (F_0), all PSII RCs are open, with Q_A fully oxidized, resulting in maximal primary photochemistry. The J and I steps of the fluorescence curve reflect the redox state of the plastoquinone pool. The J step signifies the accumulation of $Q_{A^-}Q_B$, while the I step indicates the accumulation of $Q_{A^-}Q_{B^-}$. Finally, the P step represents the activity of PSI, involving the reduction of its electron acceptors [19]. Our results showed that drought stress alters the OJIP curve by changing the fluorescence intensity at different steps. Under 25% FC condition, the fluorescence intensity at all steps was reduced compared to the control group. This reduction is attributed to a decrease in PSII and PSI antenna complexes, active reaction centers, and the size of the plastoquinone pool, which together result in diminished electron transfer capacity and reduced fluorescence emission [8]. The higher fluorescence at the O step indicates the limitations in energy trapping and photochemical processes [20]. Results from phenomenological fluxes (Fig. 4) revealed that under drought the ratio of active and inactive RCs (RC/CS) and efficiency of light absorption (ABS/CS), were significantly reduced. Consistently, the dissipation of energy from PSII (DIo/CS) was significantly increased under drought. The higher proportion of inactive RCs to active RCs resulted in diminished photon absorption, leading to a reduction in photochemical efficiency, and lowering electron production and transfer within the photosynthetic apparatus. On the other hand, the higher closed RCs serve as a dissipative sink for excitation energy, releasing it as heat. The normalized OJIP curve (Fig. 2b) showed a rise in fluorescent intensity at J and I step in both 50% and 25% of FC. Increased fluorescence at the J and I steps suggests disruptions in the redox state of the plastoquinone pool and electron careers downstream Q_B. The changes in fluorescence intensity at the P step reflect a decreased electron transfer rate in PSI electron carriers [18].

To further assess the impact of drought stress on fluorescence transient, various bands including L, K, J, H, and G bands were analyzed. The L-band emerges at 150 µs after illumination and depicts the dissociation of thylakoid structures and lower energetic connectivity in PSII. The K-band (300 µs) describes the deactivation and inhibition of the oxygen-evolving complex (OEC) [21,22] The formation of L and K bands in tomato plants under severe drought treatment can be attributed to the lower efficiency of light-harvesting complexes II (LHCII) and energy transfer to the RCs, as well as the occurrence of photoinhibition at the receptor site of PSII [23]. Our results demonstrated that severe drought stress led to the formation of J-band and H-band in tomato leaves. The J-band is linked to the electron transfer rate from Q_A to the Q_B; and the H-bans depict the redox state of the PQ pool and downstream components [24]. Formation of J and H bands signifies the impairment of electron delivery into Q_A and further delivery to Q_B and over-reduction of the plastoquinone pool, respectively. The G-band represents the reduction state of electron carriers on the acceptor side of PSI. When electron flow from plastocyanin to the final electron acceptors of PSI (such as ferredoxin and $NADP^+$) is inhibited, a positive G-band is formed [25].

Our results revealed that 50% and 25% FC significantly affected the efficiency of light reactions [φPO/ (1-φPO)], the efficiency of redox reactions [(ψO/ (1-ψO)], and the efficiency of PSI in reducing the final electron acceptors [δRo/(1−δRo)]. Reduction in the efficiency of light reactions is consistent with a lower rate of efficiency of light absorbance and trapping by PSII observed in tomato leaves under drought (Fig. 5). The fundamental parameters, the efficiency of redox reactions and the efficiency of PSI in reducing the final electron acceptors reactions were more sensitive to the progressive drought stress. Several quantum efficiencies were examined further to assess the impact points of drought on electron transport. All parameters including the quantum yield of primary photochemistry (φP_O), the quantum yield for electron transfer from Q_A to Q_B (ψ_O), the quantum yield of electron transport (φE_O), and the quantum yield necessary for the reduction of the end electron acceptors on the PSI acceptor site (φR_O), and efficiency of PSI to reduce the last electron acceptors (δRo) were negatively affected by drought. Significant reduction in φE_O, φR_O, and δRo indicates that the drought-induced damage to the photosynthetic electron transfer chain is more prominent downstream of Q_A toward PSI [26].

Our result revealed that the expression of *PetE* and *PetF* genes encoding plastocyanin (Pc) and ferredoxin (Fd), respectively, were gradually down-regulated as the drought intensified. Pc and Fd play critical roles in electron transfer within the photosynthetic electron transport chain, serving as key electron carriers. Reduction in the expression of these genes is correlated with the lower efficiency of PSI in reducing the final electron acceptors [δRo/(1−

δRo)], the quantum yield of electron transport (φE_O), and the quantum yield necessary for the reduction of the end electron acceptors on the PSI acceptor site (φR_O), and efficiency of PSI to reduce the last electron acceptors (δRo).

Numerous studies have documented that drought stress induces similar disruptions in photosynthetic efficiency across crops like maize, barley, potato, and rice [4-6, 17]. For instance, drought commonly results in reduced chlorophyll content, impaired PSII efficiency, and altered OJIP fluorescence transients, indicating structural and functional impacts on both PSII and PSI. Studies on crops like cabbage and wheat [15,23] have shown that drought can decrease the quantum yield of PSII and PSI, similar to our findings in tomatoes.

The findings of this study have important implications for agricultural practices in drought-prone regions, particularly for enhancing drought resilience in tomato cultivation. By identifying the specific sites within the photosynthetic machinery (PSII and PSI) that are highly vulnerable to drought stress, this research highlights critical targets for intervention. Strategies such as selective breeding or genetic engineering could focus on enhancing the stability of these sensitive components, especially through the maintenance of functional electron carriers like plastocyanin and ferredoxin, which play key roles in PSI efficiency. Additionally, understanding the molecular and physiological impacts of drought at different stages of water availability can inform irrigation practices aimed at minimizing stress-induced damage, thereby preserving yield.

Future research could explore several directions to deepen our understanding of drought-induced damage to the photosynthetic apparatus in tomato plants. Investigating the specific molecular mechanisms leading to PSI and PSII damage, including antioxidant responses and protein repair cycles, would clarify the biochemical changes under stress. Comparative studies across tomato varieties or related species could also identify genetic variability in drought tolerance. Additionally, examining how drought impacts downstream processes like carbon fixation and photoprotection would provide a more comprehensive view of photosynthetic responses. Genetic manipulation to sustain electron carriers (e.g., *PetE* and *PetF*) may also enhance drought resilience. Finally, understanding long-term adaptations, including potential epigenetic changes from repetitive drought exposure, could inform breeding strategies for drought-resistant cultivars.

Conclusions

The present study highlighted the detrimental effects of drought stress on the physiological and photosynthetic processes in tomato plants. A significant reduction in growth indices and pigment content was observed under drought, associated with a reduction in relative water content. The decline in chlorophyll fluorescence, particularly the alterations in the OJIP curve and formation of L, K, J, H, and G bands further confirmed the structural and functional impairments in photosynthetic machinery and disruptions in the photosynthetic electron transport chain, with reduced efficiency in both PSII and PSI drought conditions. Quantum yield parameters, such as φEO, φRO, and δRo, were significantly affected, indicating the higher vulnerability of the electron transport chain downstream of Q_B, and toward PSI and PSI donor side, confirmed by the down-regulation of *PetE* and *PetF* genes, encoding key electron carriers plastocyanin and ferredoxin. Overall, these findings highlight critical points within the photosynthetic apparatus that are particularly sensitive to water deficit. Understanding these sensitive processes can be crucial in the development of drought-resistant crop varieties and improving agricultural productivity under increasingly arid conditions.

Conflict of interest

The authors have no competing interests to declare that are relevant to the content of this article.

Consent for publication

All authors have read and approved the final manuscript for publication.

Ethics approval and consent to participate

Not applicable.

Protection of Human Subjects and Animals in Research

Not applicable.

Informed Consent in Patients and Study Participants

Not applicable.

Informed Consent

Not applicable.

Availability of data and material

The datasets gathered and analyzed during the current study are embedded in the manuscript.

Authors' contributions

Mojtaba Jafarinia and Ali Akbar Ghotbi-Ravandi contributed to the study conception and design. Material preparation and data collection were performed by Saber Nezamivand Chegini and Mojtaba Jafarinia. Data analysis was performed by Mojtaba Jafarinia and Ali Akbar Ghotbi-Ravandi. The first draft of the manuscript was written by Saber Nezamivand Cheginiand Mojtaba Jafarinia. Critical revision of the manuscript was performed by Ali Akbar Ghotbi-Ravandi.

Funding

No funds, grants, or other support were received.

References

1. Vessal S, Amirchakhmaghi N, Parsa M (2024) Variation in Morpho-Physiological Responses of Desi Chickpea (*Cicer arietinum* L.) Seedlings to Progressive Water Stress. Agrotech Ind Crops 4(3): 113-125. doi: 10.22126/atic.2024.10159.1135
2. Moradian Z, Rahdan A, Bazmakani R (2024) Germination Responses and Phenolic Compounds of *Securiger securidaca* L. Seeds under Drought and Salinity Stress Conditions. Agrotech Ind Crops. doi: 10.22126/atic.2024.10276.1139
3. Aboodeh H, Bakhshandeh A, Moradi Telavat M, Siadat SA, Moosavi SA, Alami Saeid K (2024) The Physiological Response of Rapeseed (*Brassica napus* L.) Genotypes to Drought Stress. Agrotech Ind Crops 4(1): 38-47. doi: 10.22126/atic.2024.9989.1127
4. Ahangir A, Ghotbi-Ravandi AA, Rezadoost H, Bernard F (2020) Drought tolerant maize cultivar accumulates putrescine in roots. Rhizosphere 16: 100260. doi: 10.1016/j.rhisph.2020.100260

5. Seyed Hassan Pour SM, NejadSadeghi L, Kahrizi D, Shobbar ZS (2024) Bioinformatic and Phylogenetic Investigation of WRKY Genes Involved in Drought Stress in *Camelina sativa* Plant. Agrotech Ind Crops 4(2): 65-79. doi: 10.22126/atic.2023.8830.1084
6. Bhandari U, Gajurel A, Khadka B, Thapa I, Chand I, Bhatta D, et al. (2023) Morpho-physiological and biochemical response of rice (*Oryza sativa* L.) to drought stress: A review. Heliyon 9: e13744. doi: 10.1016/j.heliyon.2023.
7. KhasheiSiuki A, Shahidi A, Dastorani M, Fallahi H, Shirzadi F (2023) Yield and Quality of Sesame (*Sesamum indicum* L.) Improve by Water Preservative Materials under Normal and Deficit Irrigation in Birjand. Agrotech Ind Crops 3(3): 121-132. doi: 10.22126/atic.2023.9167.1098
8. Ghotbi-Ravandi AA, Shahbazi M, Shariati M, Mulo P (2014) Effects of Mild and Severe Drought Stress on Photosynthetic Efficiency in Tolerant and Susceptible Barley (*Hordeum vulgare* L.) Genotypes. J Agron Crop Sci 200: 403–415. doi: 10.1111/jac.12062
9. Sharma S, Joshi J, Kataria S, Verma SK, Chatterjee S, Jain M, et al. (2020) Regulation of the Calvin cycle under abiotic stresses: an overview. In: Tripathi DK, Pratap Singh V, Chauhan DK, Sharma S, Prasad SM, Dubey NK et al. (eds) Plant Life Under Changing Environment. Academic Press: 681–717. doi: 10.1016/B978-0-12-818204-8.00030-8
10. Ghotbi-Ravandi AA, Shahbazi M, Pessarakli M, Shariati M (2016) Monitoring the photosystem II behavior of wild and cultivated barley in response to progressive water stress and rehydration using OJIP chlorophyll *a* fluorescence transient. J Plant Nutr 39: 1174–1185. doi: 10.1080/01904167.2015.1047522
11. Rao DE, Chaitanya K V. (2016) Photosynthesis and antioxidative defense mechanisms in deciphering drought stress tolerance of crop plants. Biol Plant 60: 201–218. doi: 10.1007/s10535-016-0584-8
12. Strasser RJ, Tsimilli-Michael M, Srivastava A. (2004) Analysis of the Chlorophyll *a* Fluorescence Transient. In: Papageorgiou, GC, Govindjee (eds) Chlorophyll a Fluorescence. Advances in Photosynthesis and Respiration, Springer Dordrecht pp 321-362. dio: 10.1007/978-1-4020-3218-9_12 321–362
13. Arnon DI (1949) Copper Enzymes in Isolated Chloroplasts. Polyphenoloxidase in Beta Vulgaris. Plant Physiol 24: 1–15. doi: doi:10.1104/pp.24.1.1
14. Pakdel H, Hassani SB, Ghotbi-Ravandi AA, Bernard F (2020) Contrasting the expression pattern change of polyamine oxidase genes and photosynthetic efficiency of maize (Zea mays L.) genotypes under drought stress. J Biosci 45: 73. doi: 10.1007/s12038-020-00044-3
15. Ackah E, Kotei R (2021) Effect of drought length on the performance of cabbage (*Brassica oleracea* var capitata) in the forest-savannah transition zone, Ghana. Plant Physiol Rep 26: 74–83. doi: 10.1007/s40502-020-00541-5
16. Muhammad I, Shalmani A, Ali M, Yang QH, Ahmad H, Li FB (2021) Mechanisms Regulating the Dynamics of Photosynthesis Under Abiotic Stresses. Front Plant Sci 11. doi: 1010.3389/fpls.2020.615942
17. Orsak M, Kotikova Z, Hnilicka F, Lachman J (2023) Effect of long-term drought and waterlogging stress on photosynthetic pigments in potato. Plant Soil Environ 69: 152–160. doi: 10.17221/415/2022-PSE
18. Strasser RJ, Stirbet AD (1998) Heterogeneity of photosystem II probed by the numerically simulated chlorophyll *a* fluorescence rise (O–J–I–P). Math Comput Simul 48: 3–9. doi: 10.1016/S0378-4754(98)00150-5
19. Kalaji HM, Račková L, Paganová V, Swoczyna T, Rusinowski S, Sitko K (2018) Can chlorophyll-*a* fluorescence parameters be used as bio-indicators to distinguish between drought and salinity stress in *Tilia cordata* Mill? Environ Exp Bot 152: 149–157. doi: 10.1016/j.envexpbot.2017.11.001
20. Stirbet A, Govindjee (2011) On the relation between the Kautsky effect (chlorophyll *a* fluorescence induction) and Photosystem II: Basics and applications of the OJIP fluorescence transient. J Photochem Photobiol B 104: 236–257. doi: 10.1016/j.jphotobiol.2010.12.010
21. Yusuf MohdA, Kumar D, Rajwanshi R, Strasser RJ, Tsimilli-Michael M, Govindjee et al. (2010) Overexpression of γ-tocopherol methyl transferase gene in transgenic *Brassica juncea* plants alleviates abiotic stress: Physiological and chlorophyll *a* fluorescence measurements. Biochim Biophy Acta - Bioenerge 1797: 1428–1438. doi: 10.1016/j.bbabio.2010.02.002
22. Swoczyna T, Kalaji HM, Pietkiewicz S, Borowski J (2015) Ability of various tree species to acclimation in urban environments probed with the JIP-test. Urban For Urban Green 14: 544–553. doi: 10.1016/j.ufug.2015.05.005
23. Chen W, Jia B, Chen J, Feng Y, Li Y, Chen M et al. (2021) Effects of Different Planting Densities on Photosynthesis in Maize Determined via Prompt Fluorescence, Delayed Fluorescence and P700 Signals. Plants 10: 276. doi: 10.3390/plants10020276
24. Dimitrova S, Paunov M, Pavlova B, Dankov K, Kouzmanova M, Velikova V et al. (2020) Photosynthetic efficiency of two *Platanus orientalis* L. ecotypes exposed to moderately high temperature - JIP-test analysis. Photosynthetica 58: 657–670. doi: 10.32615/ps.2020.012
25. Goussi R, Manaa A, Derbali W, Cantamessa S, Abdelly C, Barbato R (2018) Comparative analysis of salt stress, duration and intensity, on the chloroplast ultrastructure and photosynthetic apparatus in *Thellungiella salsuginea*. J Photochem Photobiol B 183: 275–287. doi: 10.1016/j.jphotobiol.2018.04.047
26. Dąbrowski P, Baczewska AH, Pawluśkiewicz B, Paunov M, Alexantrov V, Goltsev V, et al. (2016) Prompt chlorophyll *a* fluorescence as a rapid tool for diagnostic changes in PSII structure inhibited by salt stress in Perennial ryegrass. J Photochem Photobiol B 157: 22–31. doi: 10.1016/j.jphotobiol.2016.02.001